

# Dust Color Temperature and Planck Function Distribution of a Far Infrared Planetary Nebula at 90 and 140 $\mu\text{m}$ AKARI Map

S. P. Gautam<sup>1\*</sup>, A. Silwal<sup>2</sup>, and A. K. Jha<sup>1</sup>

<sup>1</sup>Central Department of Physics, Tribhuvan University, Kirtipur, Nepal.

<sup>2</sup>Patan Multiple Campus, Tribhuvan University, Lalitpur, Nepal.

## Authors' contributions

*This work was carried out in collaboration among all authors. This work is conducted under the guidance of author AKJ. There is an equal group effort of all the authors at all stages. All authors read and approved the final manuscript.*

## Article Information

### Editor(s):

- (1) Dr. Daniele Vernieri, Instituto Superior Técnico, Portugal.  
(2) Dr. Magdy Rabie Soliman Sanad, National Research Institute of Astronomy and Geophysics, Egypt.  
(3) Dr. Hadia Hassan Selim, National Research Institute of Astronomy and Geophysics, Egypt.

### Reviewers:

- (1) Abhik Kumar Sanyal, University of Kalyani, India.  
(2) Sie Long Kek, Universiti Tun Hussein Onn Malaysia, Malaysia.  
(3) Pipat Chooto, Prince of Songkla University, Thailand.  
(4) Nwaerema Peace, Ibrahim Badamasi Babangida University, Nigeria.  
(5) Xingping Wen, Kunming University of Science and Technology, China.  
Complete Peer review History: <http://www.sdiarticle4.com/review-history/57280>

Original Research Article

Received 12 April 2020

Accepted 18 June 2020

Published 06 July 2020

## ABSTRACT

We performed a study of dust color temperature and Planck function distribution of a far-infrared (FIR) planetary nebula structure (90  $\mu\text{m}$  and 140  $\mu\text{m}$ ) under the AKARI (infrared astronomy satellite developed by Japan Aerospace Exploration Agency) survey. An interesting nebular structure (major diameter  $\sim 1.57$  pc and minor diameter  $\sim 1.38$  pc) is found to lie at galactic longitude  $67.907^\circ$  and latitude  $-0.249^\circ$ , located at a distance  $\sim 1.7$  kpc was selected for the study.  $0.5^\circ \times 0.5^\circ$  AKARI all-sky map of a structure was downloaded from Sky View Virtual Observatory (<https://skyview.gsfc.nasa.gov/>) and then processed in the software ALADIN v2.503. The dust color temperature was found to lie in the range 16.99 K to 37.36 K. We found an offset of about 20 K which indicates that our structure is not independently evolved, or for the structure shaping

mechanism, the role of discrete point sources in the field of the nebula is important. We also studied the distribution of dust color temperature and Planck function along major and minor diameters. In major diameter, particles were found to be oscillating sinusoidally. This suggests that particles are not in thermal equilibrium and they are oscillating sinusoidally to get dynamical equilibrium. In minor diameter, temperature and Planck function was noticed to be linearly decreased. Further, the far-infrared spectral distribution of the structure was studied. The negative slope in the transition from 65  $\mu\text{m}$  to 160  $\mu\text{m}$  was noticed in the FIR spectral distribution of the nebula structure. Decreasing spectral distribution advocates the decrease in the number density of dust particles.

*Keywords: Planetary nebula; dust color temperature; AKARI; interstellar medium.*

## 1. INTRODUCTION

The interstellar medium (ISM) consists of matter and field, and matter contains gas and dust so that different structures such as nebula, jets, shells, filaments, arcs, lobes, loops, and cavities can be seen effectively via far-infrared telescopes. The bubbles and superbubbles produced by high-pressure events are assumed to rule the formation and evolution of these structures [1], so these FIR dust structures usually examined to be a clear hint of interaction processes in the ISM [2]. Towards the finale of their lifetime, almost all (95-98%) stars with low and intermediate initial mass ( $\sim 1-8$  solar masses) drop a significant fraction of their mass on the Asymptotic Giant Branch (AGB) in the form of massive winds, which drives them into the Planetary Nebula (PNe) stage [3]. They are widely recognized for their interesting range of shapes and morphologies. Besides being ideal laboratories for the analysis of different astrophysical processes prevailing in exceptionally exciting dilute nebulae, PNe and their progenitors are the key objects for understanding the evolution of stars [4]. The modern study of PNe is very fruitful, with many connections to adjacent fields of studies, including stellar populations, stellar structure and evolution, binary stars, radial metallicity gradients in spiral galaxies and their evolution, as well as galaxy rotation, evolution, merging, and cosmology.

Iyengar (1985) [5] studied far infrared photometric data at 12, 25, 60, and 100 microns from the Infrared Astronomical Satellite (IRAS) on forty-six optically faint planetary nebula. They determined the nebular parameters such as dust temperature, total infrared flux, infrared excesses, the mass of dust, and optical depth at 25 microns. The temperature was found to range from 60-240 K. Nick et al., (2009) [6] presented the results of a preliminary study of all known galactic planetary nebulae (included in the

Kerber 2003 catalog) which were detected by the AKARI/FIS All-sky Surveyor as recognized in the AKARI/FIS Bright Source Catalog (BSC) version  $\beta$ -1. Phillips JP, et al., (2011) [7] provided mid- and far-infrared photometry of 857 Galactic planetary nebulae using data derived from the AKARI All-Sky Survey. It was noted that the IR luminosities of the youngest PNe are comparable to the total luminosities of the central stars, and subsequently decline to  $\sim 5102 L$  where the nebular diameter is greater than 0.08 pc. That was consistent with an evolution of PNe dust opacities, and appreciable absorption in young and proto-PNe. The fall-off in dust temperatures was similar to that determined in previous studies, whilst levels of Ly heating were  $< 0.5$  of the total energy budgets of the grains. There appeared to be an evolution in the infrared excess (IRE) as nebulae expand, with the largest values occurring in the most compact PNe. Ryou O. et al., (2016) [8] performed a catalog of near-infrared low-resolution spectra of 72 galactic PNe with the infrared camera (IRC) in the post-helium phase. Spectral fitting was used to measure the intensity and equivalent width of the emission features. Jha et al., (2017) [9] studied dust mass, dust color temperature and inclination angle of the core region of KK-loops, namely G007+18, G143+07, G214-01, and G323-02, in IRIS maps. These loops were found to be located around pulsars PSR J1720-1633, PSR J0406+6138, PSR J06520142, and PSRJ1535-5848 respectively. The dust color temperature of the core region of these loops was found to lie in the range of  $19.4 \pm 1.2$  K to  $25.3 \pm 1.7$  K. Aryal et al., (2009) [10] found that the planetary nebula NGC 2899 is located at the center of a huge (14 pc  $\times$  11 pc) quadrupolar cavity, whose directions of axes coincide with the directions of the most axes of the optical planetary nebula. Aryal and Weinberger (2006) [2] detected a new infrared nebula (right ascension (R.A.) = 08 h 27 m, declination (Dec.) = +250 deg 54 m (J2000)) with an apparent size of  $\sim 140'' \times 70''$  on 60  $\mu\text{m}$  and 100  $\mu\text{m}$  IRAS maps, suggesting that the pulsar

PSRB0823+26 might be responsible for its shaping.

AKARI has been providing a database at 90  $\mu\text{m}$  and 140  $\mu\text{m}$  wavelengths. These wavelengths are extremely useful to study the interstellar dust. In this paper, the physical properties such as structure size, distribution of flux density, temperature profile, Planck function distribution, flux density variation along the major and minor axis, and far-infrared spectral distribution of a planetary nebula at galactic longitude 67.9070 and latitude -0.2490, located at a distance about 1.7 kpc [11] are best described with necessary explanations. Methods of calculation are described in section 2. In section 3, a brief description of the result and discussion will be given. Finally, we conclude our results in section 4.

## 2. METHODOLOGY

We found an interesting nebula structure for our study with possible references and coordinates query using the SIMBAD (the Set of Identifications, Measurements and Bibliography for Astronomical Data) database. A structure (major diameter  $\sim 1.57\text{pc}$  and minor diameter  $\sim 1.38\text{pc}$ ) is found to lie at galactic longitude  $67.907^\circ$  and latitude  $-0.249^\circ$ . We downloaded  $0.5^\circ \times 0.5^\circ$  AKARI all-sky map of a structure at 65, 90, 140, and 160  $\mu\text{m}$  bands from Sky View Virtual Observatory [12]. For our study, we used Aladin v2.5, one of the handy and extensively used software, developed by Center de Donne's astronomiques de Strasbourg (CDS) which is designed to reduce and analyze the data collected from the ground-based and space telescopes covering all wavelength regions. Information regarding the energy spectrum, relative flux density with coordinates of each pixel, different types of contour maps, longitude and the latitude of the desired astronomical structure can be obtained. After the selection of interesting nebular structure, FITS (Flexible Image Transport System) images at different bands of AKARI were downloaded. Each pixel of the FITS image of our region of interest was analyzed using software Aladin v2.5. Various sources of energy around the region of interest obtained from SIMBAD possibly increase the flux of region of interest. Flux density obtained from 90  $\mu\text{m}$  and 140  $\mu\text{m}$  images were corrected by subtracting it with the background. We described a method of calculation of dust color temperature, Planck function, and size of the structure.

### 2.1 Dust Color Temperature

We adopted the method proposed by Schnee et al., [13] and Dupac et al. [14], for the calculation of dust color temperature. The expression for the dust color temperature in 60 and 100  $\mu\text{m}$  IRAS (Infrared Astronomical Satellite) map is given by,

$$T_d = \frac{-96}{\ln\{R \times 0.6^{(3+\beta)}\}},$$

$$\text{where the flux ratio } R = \frac{F(60\mu\text{m})}{F(100\mu\text{m})} \quad (2.1)$$

$F(60\mu\text{m})$  and  $F(100\mu\text{m})$  are the flux densities in 60  $\mu\text{m}$  and 100  $\mu\text{m}$  respectively.

The background-corrected flux density at each pixel inside the region of interest was measured from the AKARI 140  $\mu\text{m}$  image using the software Aladin v2.5. Similarly, the corresponding flux densities were measured from the AKARI 90  $\mu\text{m}$  image. Using the ratio of the flux density in the AKARI 90  $\mu\text{m}$  to the flux density in the AKARI 140  $\mu\text{m}$ , as in IRAS survey, the expression for dust color temperature for AKARI map becomes [1],

$$T_d = \frac{-57}{\ln\{R \times 0.6^{(3+\beta)}\}},$$

$$\text{where the flux ratio } R = \frac{F(90\mu\text{m})}{F(140\mu\text{m})} \quad (2.2)$$

$F(90\mu\text{m})$  and  $F(140\mu\text{m})$  are the flux densities at 90  $\mu\text{m}$  and 140  $\mu\text{m}$  respectively. Eq. (2.2) was used for calculation of the dust color temperature. The spectral emissivity index ( $\beta$ ) depends on dust grain properties like composition, size, and compactness. For a pure blackbody would have  $\beta = 0$ , the amorphous layer-lattice matter has  $\beta \sim 1$ , and the metals and crystalline dielectrics have  $\beta \sim 2$  which was used in our calculations [15].

### 2.2 Planck Function

The value of Planck function depends on the wavelength (frequency), and hence the temperature. It is an important parameter to study dust within the structure. In 1900, Planck proposed a relation which is named as Planck function, given by

$$B(\nu, T) = \frac{2h\nu^3}{c^2} \left[ \frac{1}{\exp\left(\frac{h\nu}{kT}\right) - 1} \right] \quad (2.3)$$

where,  $h$  = Planck constant =  $6.62 \times 10^{-34}$  Js,  $c$  = velocity of light =  $3 \times 10^8$   $\text{ms}^{-1}$ ,  $\nu$  = frequency at

which the emission is observed =  $2.14 \times 10^{12}$  Hz,  $k$  = Boltzmann constant =  $1.38 \times 10^{-23}$  JK<sup>-1</sup>, and  $T$  = temperature of each pixel.

### 2.3 Dust Size

The major and minor diameter of the structure can be calculated by using a simple expression i.e. [9],

$$L = D \times \theta \quad (2.4)$$

where  $D$  is the distance to the structure and  $\theta$  is the pixel size (in radian).

### 3. RESULTS AND DISCUSSION

We separated the maximum flux regions drawing contours at 90 and 140  $\mu$ m AKARI images using Aladin v2.5 which is shown in Fig. 1(a) and 1(b). The flux regions were covered within the contour level 187 and 54. The distribution of flux density

at 90  $\mu$ m and 140  $\mu$ m, flux density within the contour level with R.A. and Dec., were plotted in the contour map by using ORIGIN 9.0 as shown in Fig. 1(c) and 1(d). The graph shows that all the fluxes from minimum to maximum appeared within the contour level. The maximum flux region was found to lie at the center.

Flux density at each pixel was measured in different bands of the AKARI map. Fluxes at 90  $\mu$ m and 140  $\mu$ m were plotted with the help of ORIGIN 9.0 to see the distribution of flux density within the core region of the structure as shown in Fig. 2(a). From the plot, we can see that flux variation in both higher and lower flux was linearly distributed. The slope of the line was found to be 0.61 with the correlation coefficient  $R = 0.91$ . The significance of the linear fit in the flux variation is that it gives us a ratio of lower to higher flux which can help us to calculate the average dust color temperature of the structure.

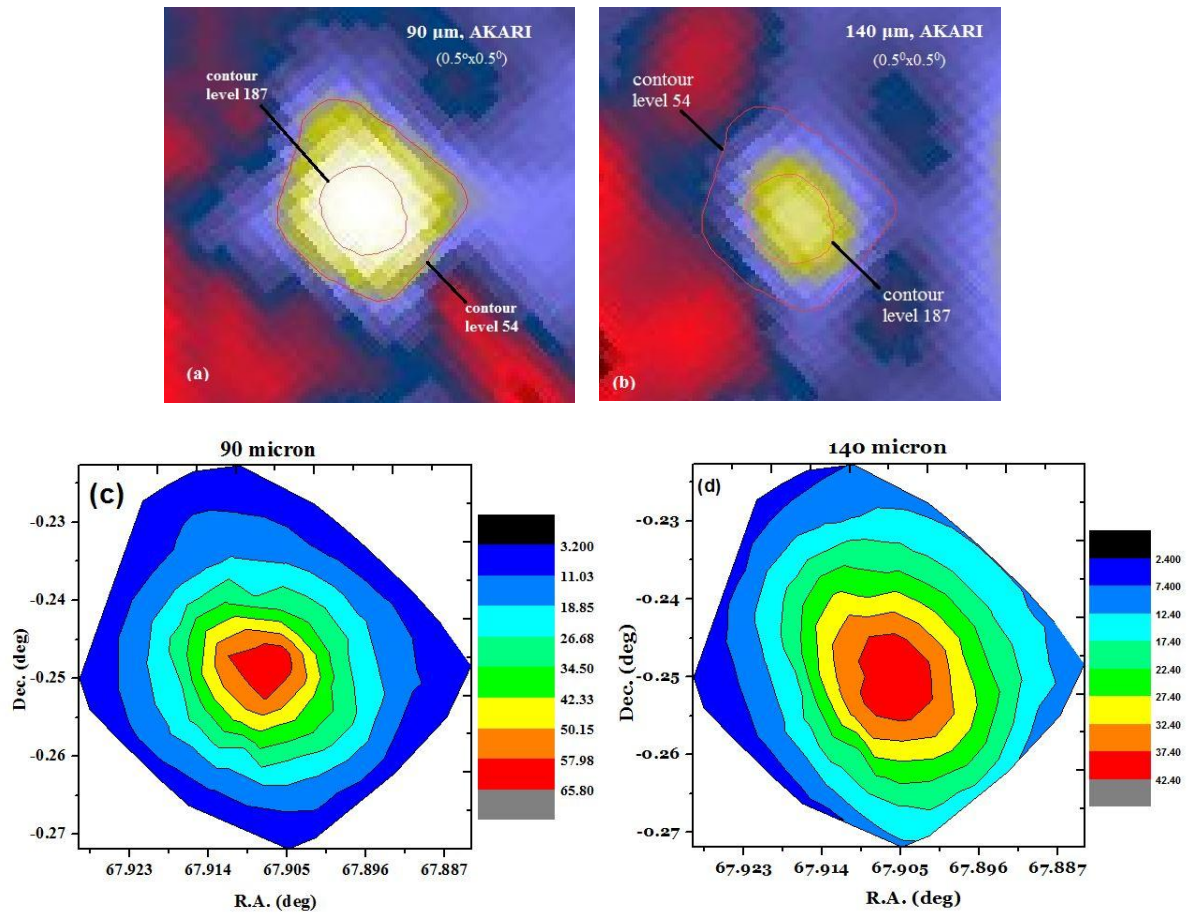


Fig. 1. (a)  $0.5^\circ \times 0.5^\circ$  FITS image of the structure at 90  $\mu$ m AKARI map. (b)  $0.5^\circ \times 0.5^\circ$  FITS image of the structure at 140  $\mu$ m AKARI map. (c) Contour map at 90  $\mu$ m flux density. (d) Contour map at 140  $\mu$ m flux density where the PNe is located at R.A = 67.907°, Dec. = -0.249° (Galactic)

The ratio of fluxes at 90 and 140  $\mu\text{m}$  at each pixel was measured using the software Aladin v2.5 for the estimation of dust color temperature at each pixel of the structure. Equation (2.2) was used for the calculation of dust color temperature. The plot of the variation of temperature with corresponding R.A. and Dec. is shown in Fig. 2(b). The graph shows that temperature distributions were found in clusters of separate layers but an interestingly maximum temperature region was shifted from the maximum flux density which is an unusual behavior. Such type of nature is found due to external factors possibly due to pulsar wind, AGB wind, white dwarfs, etc around the structure. Fig. 2(c) represents the Gaussian fitting of temperature versus the number. We found the Gaussian center at 24.67 K with standard error 0.73 K. The average temperature of the structure was found to be 20.91 K using the slope of the best-fitted curve obtained from Fig. 2(a). The

minimum and maximum temperature in the region of interest was found in the range 16.99 K to 37.36 K. We got an offset of about 20 K which indicates that our structure is not independently evolved or, for the structure shaping mechanism, the role of discrete point sources in the field of the nebula is important [1].

We plotted the contour map of Planck function (in  $\text{Wm}^{-2}\text{Sr}^{-1}\text{Hz}^{-1}$ ) within the structure, which is shown in Fig. 2(d). The Planck function shows the spectral density of electromagnetic radiation emitted by a body at a temperature. The spectral density shows how the energy of a signal or a time series is distributed with frequency. The contour separates the different spectral densities whereas the color indicates them. The plot shows that the spectral densities were found to be uniformly distributed in different layers, but the maximum density was found to lie away from the center.

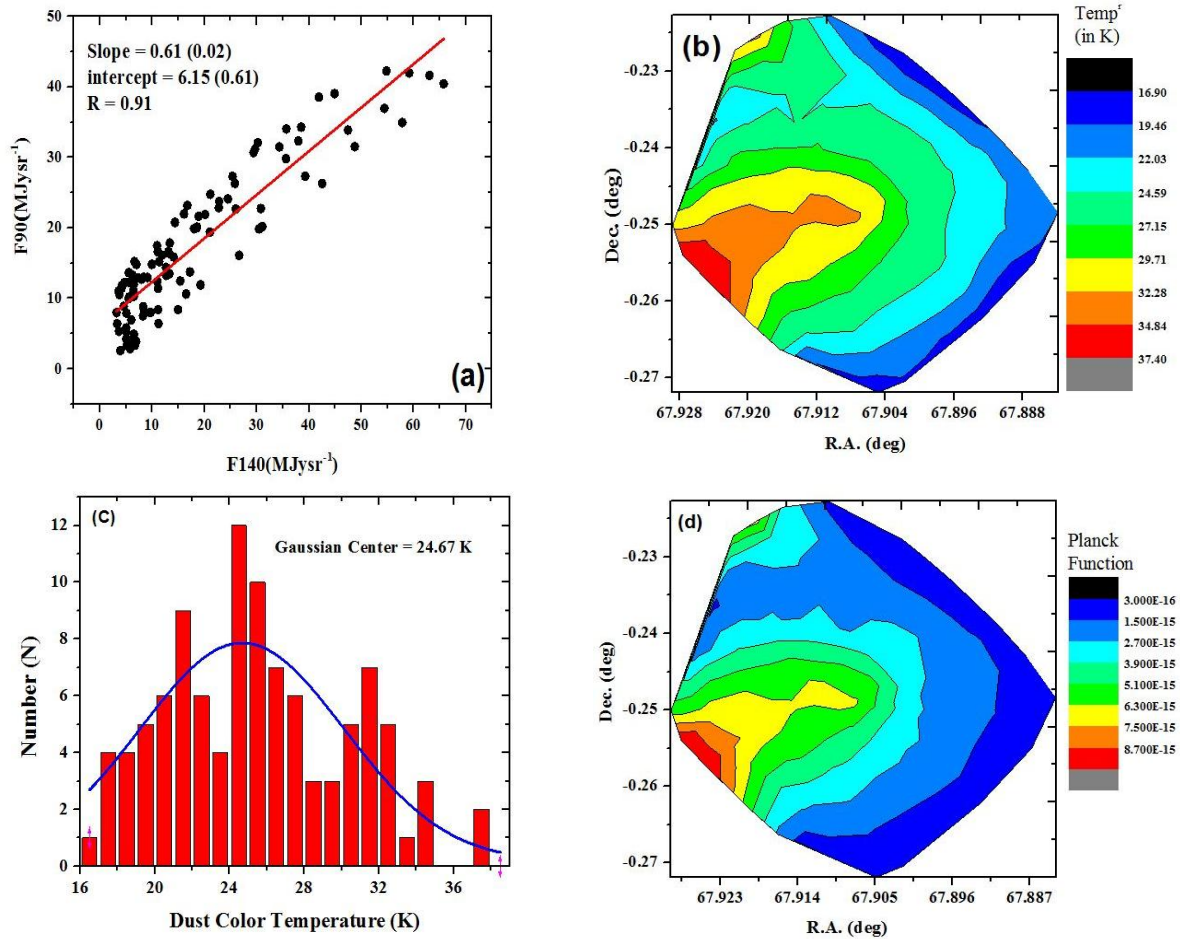
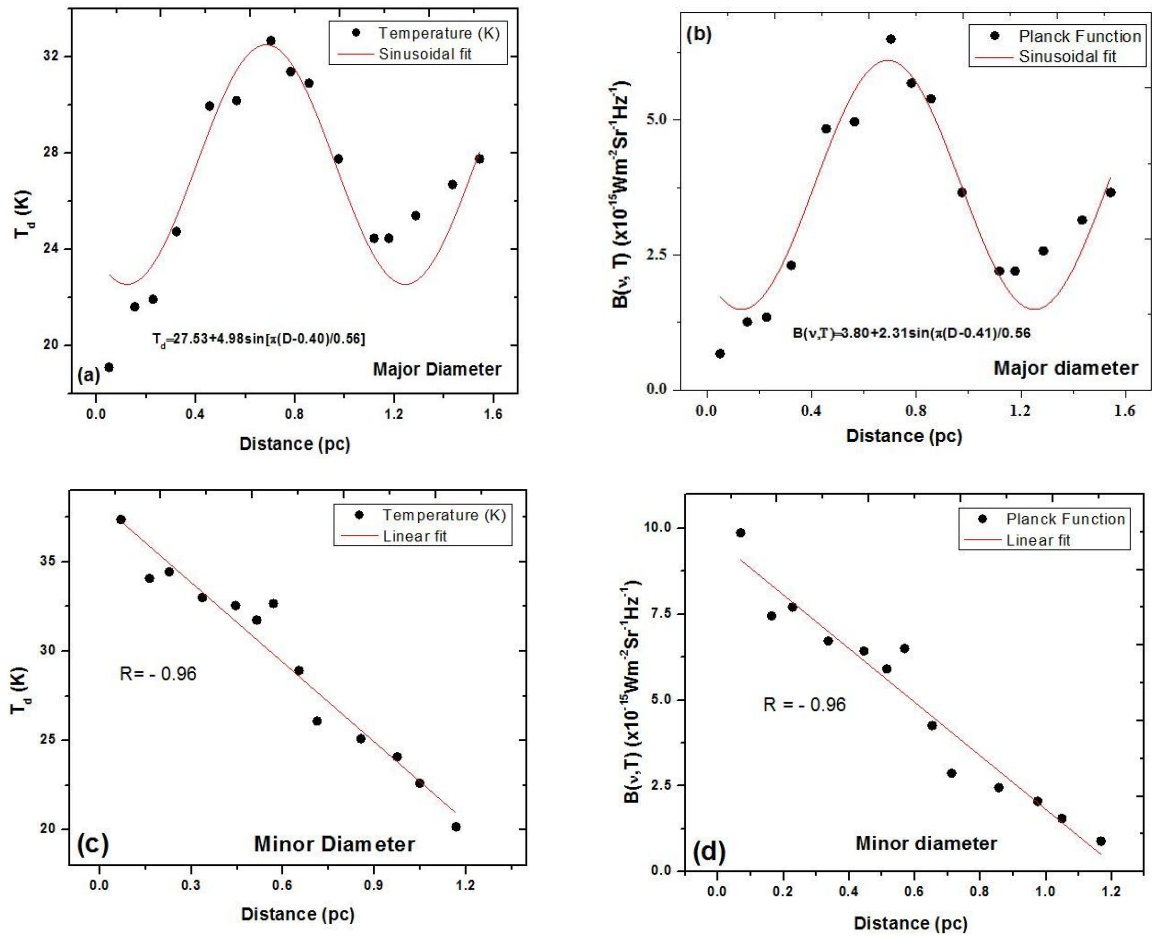
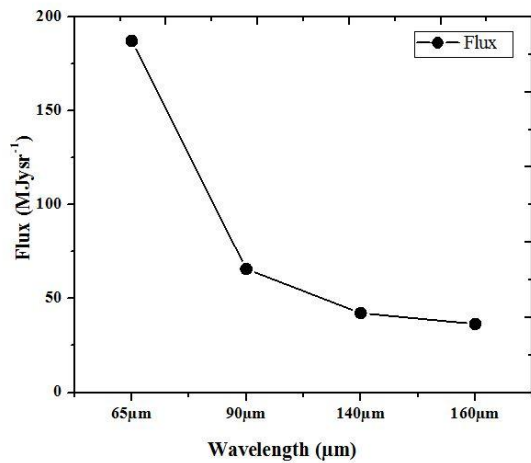


Fig. 2. (a) The 160  $\mu\text{m}$  versus 90  $\mu\text{m}$  flux density in the region of interest. (b) Contour map of dust color temperature (c) Gaussian fit of dust color temperature. (d) Contour map of Planck function where the PNe which is located at R.A = 67.907°, Dec. = -0.249° (Galactic)





**Fig. 3. Sinusoidal fit of the scattered plot between distance and temperature in major diameter. (b) Sinusoidal fit of the scattered plot between distance and Planck function in major diameter. (c) Linear fit of the scattered plot between distance and temperature in minor diameter. (d) Linear fit of the scattered plot between distance and Planck function in minor diameter of a nebula structure located at R.A = 67.907°, Dec. = -0.249° (Galactic)**



**Fig. 4. Spectral distribution of a nebula structure**

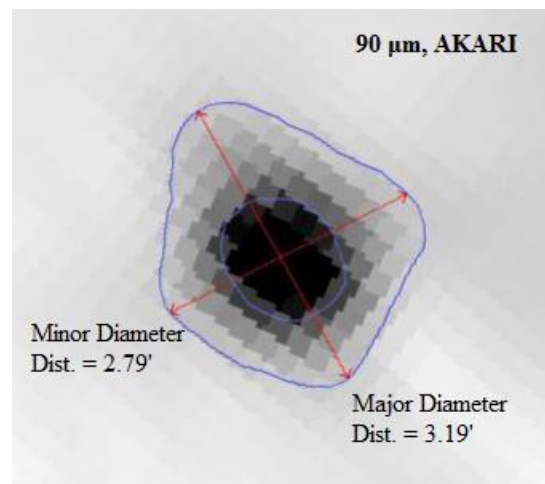


**Fig. 5. Major and minor diameter of the nebula structure**

Fig. 3(a) and (b) show the distribution of temperature and Planck function respectively along major diameter in which the temperature and Planck function of dust particles was found to be oscillating. We found that the particles were oscillating sinusoidally. This suggests that particles are not in thermal equilibrium and they are oscillating sinusoidally to get dynamical equilibrium [14]. In the minor diameter, dust color temperature and Planck function was found to decrease linearly.

Spectral distribution is a plot between wavelength and flux density. We studied the spectral distribution of the far-infrared nebula at galactic longitude  $67.907^\circ$  and latitude  $-0.249^\circ$  which is shown in Fig. 4. We found negative slopes in the transition from  $65 \mu\text{m}$  to  $160 \mu\text{m}$  in the spectral distribution of the nebula structure. The minimum negative transition was obtained from  $140 \mu\text{m}$  to  $160 \mu\text{m}$ . Decreasing spectral distribution suggests a decrease in the number density of dust particles [16]. Using the distance tool available in the software Aladin v2.5, we measured the distance in major and minor diameter of the nebula structure taking maximum flux region as a center as shown in Fig. 5. Using equation 2.4, we calculated the size of the nebula structure. We used the distance (D)  $1.7 \text{ kpc}$  [11] for our structure. The major and minor diameter of the structure was found to be  $1.57 \text{ pc}$  and  $1.38 \text{ pc}$  respectively.

#### 4. CONCLUSION

Dust color temperature and Planck function distribution of the planetary nebula at galactic longitude  $67.907^\circ$  and latitude  $-0.249^\circ$  in the AKARI map was studied. Further, flux density variation, temperature variation, and Planck function along the major and minor diameter, size of the structure, and spectral distribution of a structure was studied using the software Aladin v2.5. The plot between flux density in  $90 \mu\text{m}$  and  $140 \mu\text{m}$  AKARI suggests that the flux variation in both higher and lower flux was linearly distributed with the slope of the line  $0.61$ , and the correlation coefficient  $0.91$ . Average dust color temperature was found to be  $20.91 \text{ K}$  at our region of interest ranging from  $16.99 \text{ K}$  to  $37.36 \text{ K}$  with the offset of about  $20 \text{ K}$  which suggests that our structure is not independently evolved or the role of discrete point sources in the field of the nebula is important for the structure shaping mechanism. From the plot of Planck function distribution, spectral densities were found to be uniformly distributed in different layers, but the maximum

density was found to lie away from the center. Dust color temperature and Planck function distribution along major and minor diameters were also studied. In major diameter, particles were found to be oscillating sinusoidally. This suggests that particles are not in thermal equilibrium and they are oscillating sinusoidally to get dynamical equilibrium. In minor diameter, we witnessed the linear decrease in dust color temperature and Planck function. The size of the nebular structure was calculated as  $1.57 \text{ pc} \times 1.38 \text{ pc}$ . From the study of the spectral distribution of FIR nebula structure, a negative slope in the transition from  $65 \mu\text{m}$  to  $160 \mu\text{m}$  was noticed. Decreasing spectral distribution, as accounted by the negative slope during the transition, points out the decrease in the number density of dust particles within the structure. This study serves as a baseline to carry out further studies about the shaping mechanism of Interstellar Medium.

#### DISCLAIMER

The products used for this research are commonly and predominantly use products in our area of research and country. There is absolutely no conflict of interest between the authors and producers of the products because we do not intend to use these products as an avenue for any litigation but for the advancement of knowledge. Also, the research was not funded by the producing company rather it was funded by the personal efforts of the authors.

#### ACKNOWLEDGEMENTS

We are thankful to the Central Department of Physics for providing previous thesis books which were very helpful for the literature. This research has made use of Sky View Virtual Observatory, Aladin v2.5, SIMBAD database, and ORIGIN9.0.

#### COMPETING INTERESTS

Authors have declared that no competing interests exist.

#### REFERENCES

1. Jha AK, Aryal B. Dust color temperature distribution of two FIR cavities at IRIS and AKARI maps. *J. Astrophys. Astr.* 2018; 39(24):7. Available: <https://doi.org/10.1007/s12036-018-9517-6>

2. Aryal B, Weinberger R. A new large high latitude cone-like far-IR Nebula. *A&A*. 2006;448(1):213-219. Available:<https://doi.org/10.1051/0004-6361:20042440>
3. Aryal B, Weinberger R. Study of mass-loss in the planetary nebula NGC 1514. *Scientific World*. 2007;5(5):6-9. DOI: 10.3126/sw.v5i5.2647
4. Weinberger R, Kerber F. Planetary nebulae: Understanding the physical and chemical evolution of dying stars. *Science*. 1997;276:1382-1386. DOI: 10.1126/science.276.5317.1382
5. Iyengar KVK. Study of IRAS observations of faint planetary nebulae. *A&A*. 1986; 158(1-2):89-96. (Bibcode: 1986A&A...158...89I).
6. Nick C, Manchado A, Garcia-Lario P, Szczerba R. Galactic planetary nebulae in the AKARI far-infrared surveyor bright source catalog. *ASP Conference Series*, University of Tokyo, Tokyo, Japan. 2009; 418:439. (Bibcode: 2009ASPC..418..439C).
7. Phillips JP, Marquez-Lugo RA. Mid- and far-infrared photometry of galactic planetary nebulae with the AKARI all-sky survey. *RMxAA*. 2011;47(1):83-112. (Source: arXiv:1102.0526v2)
8. Ryou O, Takashi O, Itsuki S, Mikako M, Hidehiro K. AKARI/IRC near-infrared spectral atlas of galactic planetary nebulae. *The Astronomical Journal*. 2016; 151(93):28. DOI: 10.3847/0004-6256/151/4/93
9. Jha AK, Aryal B, Weinberger R. A study of dust color temperature and dust mass distributions of four far-infrared loops. *RMxAA*. 2017;53:467-476. (Bibcode: 2017RMxAA..53..467J).
10. Aryal B, Rajbahak C, Weinberger R. Planetary nebulae NGC 6826 and NGC 2899: Early Aspherical Mass Loss? *Ap&SS*. 2009;323(4):323-327. DOI: 10.1007/s10509-009-0076-9
11. Tajitsu A, Tamura S. A new distance indicator to galactic planetary nebulae based upon IRAS Fluxes. *The Astronomical Journal*. 1998;115:1989-2008. DOI: 10.1086/300315
12. Skyview Virtual Observatory. The National Aeronautics and Space Administration (NASA). Available:<https://skyview.gsfc.nasa.gov/>
13. Schnee SL, Ridge NA, Goodman AA, Jason GL. A complete look at the use of IRAS Emission Maps to Estimate Extinction and Dust Temperature. *The Astrophysical Journal*. 2005;634:442-450. DOI: <https://doi.org/10.1086/491729>
14. Dupac X, Bernard JP, Boudet N, Giard M, Lamarre JM, Meny C, et al. Inverse temperature dependence of the dust submillimeter spectral index. *Astronomy & Astrophysics*. 2003;404:L11-L15. DOI:<https://doi.org/10.1051/0004-6361:20030575>
15. Gautam AK, Aryal B. A study of four low-latitude ( $|l| < 100$ ) Far-infrared Cavities. *Journal of Astrophysics and Astronomy*. 2019;40(2):16. DOI: 10.1007/s12036-019-9578-1
16. Gautam AK, Aryal B. Study of dust color temperature and visual extinction distribution of a far infrared cavity at 60 and 100  $\mu\text{m}$  IRAS Map around the AGB Star at Galactic Latitude  $8.6^\circ$ . *BIBECHANA*. 2020;17:42-49. Available:<https://doi.org/10.3126/bibechana.v17i0.25839>

© 2020 Gautam et al.; This is an Open Access article distributed under the terms of the Creative Commons Attribution License (<http://creativecommons.org/licenses/by/4.0>), which permits unrestricted use, distribution, and reproduction in any medium, provided the original work is properly cited.

*Peer-review history:*  
The peer review history for this paper can be accessed here:  
<http://www.sdiarticle4.com/review-history/57280>